

## Maternal Hyperglycemia Induces Changes in Gene Expression and Morphology in Mouse Placentas

Molly Eckmann MD<sup>1</sup>, Quanhu Sheng PhD<sup>2</sup>, Scott Baldwin H MD, PhD<sup>3</sup> and Rolanda L. Lister MD<sup>4\*</sup>

<sup>1</sup>Vanderbilt University Medical School, 1211 Medical Center Dr, Nashville, TN 37232, United States.

<sup>2</sup>Department of Biostatistics, Vanderbilt University Medical Center, 1211 Medical Center Dr, Nashville, TN 37232, United States.

<sup>3</sup>Division of Pediatric Cardiology, Department of Pediatrics, Vanderbilt University Medical Center, 1211 Medical Center Dr, Nashville, TN 37232, United States.

<sup>4</sup>Division of Maternal Fetal Medicine, Department of Obstetrics and Gynecology, Vanderbilt University Medical Center, Nashville, TN 37080, United States.

### \*Correspondence:

Rolanda L. Lister, MD, Division of Maternal Fetal Medicine, Department of Obstetrics and Gynecology, Vanderbilt University Medical Center, B1100 Medical Center North, Nashville, TN 37232, United States, Tel: (615)343-5700 ext 64817, Cell: (615) 668-5171.

Received: 15 December 2020; Accepted: 07 January 2021

**Citation:** Eckmann M Sheng Q, Baldwin SH, et al. Maternal Hyperglycemia Induces Changes in Gene Expression and Morphology in Mouse Placentas. *Gynecol Reprod Health*. 2020; 4(4): 1-15.

### ABSTRACT

**Background:** Pregestational diabetes complicates one million pregnancies in the United States and is associated with placental dysfunction. Placental dysfunction can manifest as stillbirth, spontaneous abortions, fetal growth restriction, and preeclampsia in the mother. However, the underlying mechanisms of placental dysfunction are not well understood.

**Objective:** We hypothesize that maternal hyperglycemia disrupts cellular processes important for normal vascular development and function.

**Study Design:** Hyperglycemia, defined as a non-fasting glucose concentration of >250 mg/dL was induced in eight-week-old female CD1 mice by injecting a one-time intraperitoneal dose of 150mg/kg streptozotocin. Control mice received an equal volume of normal saline. Hyperglycemic and control females were mated with CD-1 males. At Embryonic Day 17.5, the pregnant mice were euthanized. Sixty-eight placentas were harvested from the six euglycemic dams and twenty-six placentas were harvested from three hyperglycemic dams. RNA was extracted from homogenized placental tissue (N=12/group; 2-4 placentas per litter of each group). Total RNA was prepared and sequenced. Differentially expressed genes that were >2-fold change was considered significant. Placentas (9-20/group) were fixed in paraffin wax and sectioned at 6  $\mu$ m. Cross-sectional areas of placental zones were evaluated using slides stained for hematoxylin and eosin, glycogen, collagen, proliferation and apoptosis. Quantification of staining intensity and percent positive nuclei was done using Leica Image Hub Data software. Data were compared between the control and experimental group using t-tests. Values of  $p < 0.05$  were considered to be statistically significant.

**Results:** The average maternal blood glucose concentrations for control and diabetic dams were 112 $\pm$ 24 and 473 $\pm$ 47 respectively ( $p < 0.0001$ ). A higher rate of resorptions was noted in the hyperglycemia exposed placentas compared to euglycemic exposed placentas (24% vs 7%;  $p = 0.04$ ). A total of 24 RNA libraries (12/group) were prepared. Placentas from hyperglycemic pregnancies exhibited 1374 differentially expressed genes (DEGs). The 10 most significantly differentially expressed genes are *Filip 1*, *Prom 2*, *Fam 78a*, *Pde4d*, *Pou3f1*, *Kcnk5*, *Dusp4*, *Cxcr4*, *Slc6a4* and *D430019H16Rik*. Their corresponding biologic functions are related to chemotaxis, ossification, cellular and vascular development. Histologically, we found that hyperglycemia exposed placentas demonstrated increased proliferation, apoptosis, and glycogen content and decreased collagen deposition.

**Conclusion:** There was a higher rate of resorptions in the pregnancies of hyperglycemic dams. Pregestational diabetes resulted in significant changes in placental morphology, including increased glycogen content in the spongiotrophoblast, decreased collagen deposition, increased apoptosis and proliferation in the junction zone. Maternal diabetes causes widespread disruption in multiple cellular processes important for normal vascular development and sets the platform for placenta dysfunction.

## Keywords

Apoptosis, Collagen staining, Differentially expressed genes, Euglycemia, Genome wide mRNA expression, Hyperglycemia, Maternal diabetes, Placenta dysfunction, Proliferation, Streptozotocin, Vascular dysfunction.

## Introduction

Pregestational diabetes complicates approximately one million pregnancies in the United States [1]. It is associated with placental dysfunction which manifests as spontaneous abortions, fetal growth restriction, stillbirth, and preeclampsia in the mother. It is seen more often in T1DM than in T2DM or gestational diabetes (GDM) [1-4]. Despite the known vascular complications of diabetes in and outside of pregnancy, the genetic underpinnings of diabetes-associated placental angiogenic dysfunction are not well understood. This study examines the unbiased genome wide expression profile of murine pregnancies exposed to maternal hyperglycemia compared to euglycemia. We hypothesized that pregestational maternal hyperglycemia be cause's abnormal gene expression in genes important to vascular development and function and manifest as embryonic demise and abnormal placental pathology in mice.

Identification of novel genes that are differentially expressed in the placentas exposed to maternal diabetes once corroborated in human placentas could serve as targets for intervention to reduce diabetes related placental dysfunction. Murine placentas are useful models for investigating human placental disease as there are analogous zones that correspond to the human maternal fetal interface that facilitate gas and nutrient exchange [5]. The mature murine placenta consists of four distinct zones (Figure 1). The outermost layer is the decidua (D) and consists of the maternal side of the placenta. It is separated from the adjacent junctional zone (JZ) by a layer of trophoblast giant cells or spongiotrophoblasts, which, like the cytotrophoblasts in humans, is responsible for implantation into the uterus and is the location for significant glycogen deposition [6,7]. The labyrinth zone (LZ), is analogous to chorionic villi in humans and is responsible for gas and nutrient exchange between the fetus and mother [6]. Finally, the chorionic plate (CP) is the location of the entry of fetal blood vessels into the placenta[6].

In this study, pregestational hyperglycemia was induced in mice using streptozocin. Streptozocin selectively eliminates the insulin producing beta islet cells of the pancreas rendering the mouse hyperglycemic [8]. We chose this model of hyperglycemia because it is an efficient and highly reproducible way to induce diabetes without compromising fertility of the animal [9]. Additionally, mothers with T1DM are more likely to have worse pregnancy outcomes including preterm birth, preeclampsia worse glycemic control and fetal demise compared to T2DM and GDM [10,11]. Embryonic day 17.5 was chosen as it corresponds to late gestation where placenta mediated pathologies are more pronounced [12]. Although the mechanism of insulin deficiency is not antibody mediated, the reduction of circulating insulin renders the animal most similar to T1DM [8]. Placental tissue was collected and analyzed with whole genome RNA sequencing and immunohistochemistry. The aims are twofold: first, to utilize RNA sequencing to gain insight into the genetic basis of hyperglycemia-induced placental dysfunction; and second, to evaluate the histological changes in hyperglycemic placentas as they relate to biological pathways and functions enriched within the identified set of differentially expressed genes. These findings will allow us to gain insight into the mechanisms underlying placental dysfunction in patients with pregestational T1DM.

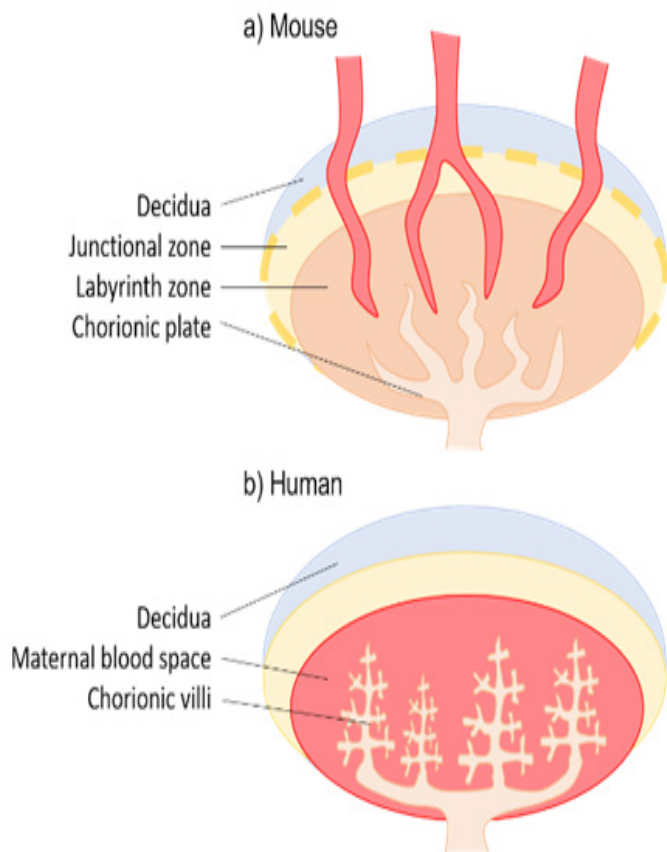


**Figure 1:** Mouse versus human placenta morphology. The labyrinth and junctional zone in mice placentas facilitate similar functions as the chorionic maternal interface in human placentas.

## Materials and Methods

### Husbandry

Mice were obtained by approved vendors and housed in our animal facility. Animals were housed in micro isolation colorless cages and given food and water ad libitum for blood glucose measurements. Housing rooms were temperature controlled with 12 hours alternating light and dark cycle. All mouse experiments were performed according to the guidelines of the National Institute of Health and the protocol approved by the Institutional Animal Care and Use Committee of Vanderbilt University Medical Center.

---

## Experimental model

Hyperglycemia was induced in eight-week-old female CD1 mice by injecting 150mg/kg streptozotocin intraperitoneally [13]. Control mice received an equal volume of normal saline. Blood glucose was measured at 10 weeks of age using the Abbott Precision Extra Blood Glucose and Ketone Monitoring System (Abbott, Alameda, USA) prior to mating. Hyperglycemia was defined as a random blood glucose level greater than or equal to 250 mg/dL [14]. Mice were mated at 10 weeks of age and checked daily for vaginal plugs. Noon on the day of observing vaginal plugs was designated as embryonic day (E) 0.5. At E17.5 days after the appearance of a vaginal plug, pregnant mice were transferred out of the animal housing facility to the cardiovascular core facility for blood pressure measurements.

## Phenotype analysis

Blood pressure measurements were obtained using the BP-2000 Blood Pressure Analysis System (Visitech Systems, Apex, USA) via the tail-cuff method [15]. This system utilizes volume-pressure recording technology to detect changes in tail volume that correspond to systolic and diastolic pressures and calculates mean arterial pressure (MAP) during each measurement cycle. Unanesthetized mice were placed in plastic holders. Our protocol consisted of 5 acclimation cycles and 5 measurement cycles. Animals were then transferred to the animal dissection room for sacrifice. After the animals were euthanized, urine samples were also collected at time of sacrifice. Urinary albumin was measured using the Albuwell M kit (Exocell, Philadelphia, USA). Urinary creatinine was measured using the Creatinine Companion murine ELISA kit (Exocell, Philadelphia, USA). A cesarean was performed, and the placentas were harvested from the uterine horns of each dam.

## Placental gene expression analysis

RNA was extracted from homogenized placental tissue (12 samples/group; 2-4 placentas/litter in each group) using the commercial Qiagen RNA extraction kit (Qiagen, Hilden, Germany) per manufacture guidelines. Total RNA was prepared using the Illumina Tru-Seq RNA sample prep kit (Illumina, San Diego, USA), and sequencing was conducted on the Illumina HiSeq 2500 (Illumina, San Diego, USA). Reads were trimmed to remove adapter sequences using Cutadapt v1.16 [16] and aligned to the GENCODE GRCm38.p5 genome using STAR v2.5.3a [17]. GENCODE vM16 gene annotations were provided to STAR to improve the accuracy of mapping. Quality control on both raw reads and adaptor-trimmed reads was performed using FastQC ([www.bioinformatics.babraham.ac.uk/projects/fastqc](http://www.bioinformatics.babraham.ac.uk/projects/fastqc)). FeatureCounts v1.15.2 [18] was used to count the number of mapped reads to each gene. Significantly differential expressed genes with FDR-adjusted  $p$ -value  $< 0.05$  and absolute fold change  $> 2.0$  were detected by DESeq2 (v1.18.1) [19]. Heatmap3 was used for cluster analysis and visualization [20]. Genome Ontology and KEGG pathway over-representation analysis was performed on differentially expressed genes using the Web Gestalt R package [21].

## Placental morphology

Placentas (9-20/group) were fixed in paraffin wax and sectioned at 6  $\mu\text{m}$ . Cross-sectional areas of placental zones were evaluated using slides stain with hematoxylin and eosin (H&E). Cross-sectional areas of the chorionic plate (CP), labyrinth zone (LZ), junctional zone (JZ), and decidua (D) were measured. Relative magnitude of glycogen deposition was determined by measuring the total area of cells with clear cytoplasm in the JZ [22].

## Collagen staining

Collagen deposition was determined using Maisson's trichrome blue stain protocol [23]. Briefly, slides were deparaffinized and incubated in Bouin's fluid overnight. Slides were then stained with hematoxylin, rinsed and stained with trichrome stain, gomori One-Step, Aniline blue for 20 minutes and dipped in Acetic Acid 0.5%. Slides were then dehydrated, cleared and cover slipped. Collagen deposition was quantified as the percent area of trichrome blue positive of each zone.

## Apoptosis assay

Immunohistochemistry was performed with anti-caspase 3. Slides were placed on the Leica Bond Max IHC stainer. Heat induced antigen retrieval was performed using Epitope Retrieval 2 solution for 15 minutes. Slides were placed in a Protein Block (Ref# x0909, DAKO) for 10 minutes. Slides were incubated with cleaved Caspase-3 (Cat. 9664, Cell Signaling) for one hour at a 1:300 dilution. The Bond Polymer Refine detection system was used for visualization. Slides were the dehydrated, cleared and cover slipped. Apoptosis was quantified as the percent area of each zone with positive immune reactivity.

## Proliferation assay

Slides were placed on the Leica Bond Max IHC stainer. All steps besides dehydration, clearing and cover slipping are performed on the Bond Max. Slides are deparaffinized. Heat induced antigen retrieval was performed on the Bond Max using their Epitope Retrieval 2 solution for 20 minutes. Slides were placed in a Protein Block (Ref# x0909, DAKO, Carpinteria, CA) for 10 minutes. The sections were incubated with anti-Ki67 (Catalog #12202S, Cell Signaling Technology, Danvers, MA) diluted 1:300 for one hour. The Bond Refine Polymer detection system was used for visualization. Slides were the dehydrated, cleared and cover slipped. Proliferation was quantified as the percent of Ki67 positive nuclei per placental zone.

## Image analysis

Image analysis was performed using the Leica Digital Image Hub (Leica Bio systems, Wetzlar, Germany). Differentially expressed genes, collagen staining intensity and glycogen content were compared between the control and experimental group using  $t$ -tests. Values of  $p < 0.05$  were considered to be statistically significant.

## Results

### Induction of hyperglycemia and pregnancy phenotype outcomes

Hyperglycemia was successfully induced in mice who received STZ. At 10 weeks of age, average random blood glucose level was  $112 \pm 24$  mg/dL in the control group and  $473 \pm 47$  mg/dL in the experimental group ( $p < 0.0001$ ) (see supplemental data-Table 1). Hyperglycemic placentas weighed almost twice as much as euglycemic placentas ( $0.14 \pm 0.03$  vs.  $0.09 \pm 0.02$ ;  $p < 0.01$ ). Hyperglycemic pregnancies had a significantly higher rate of resorption (24% vs. 7%;  $p = 0.04$ ), but similar number of embryos per day (Table 1) (Figure 2). Shows a significantly higher rate of resorptions in the hyperglycemic pregnancies versus euglycemic pregnancies. Additionally, when evaluating the phenotype of preeclampsia, the hyperglycemic dams trended to an elevated urine protein to creatinine ratio; however they did not demonstrate hypertension. (See supplemental data-Table 1).

Parameter	Euglycemia (n=68)	Hyperglycemia (n=26)	P-value
Pup weight (g)	$0.73 \pm 0.05$	$0.76 \pm 0.07$	0.59
Placenta weight (g)	$0.09 \pm 0.02$	$0.14 \pm 0.03$	$< 0.01$
Placenta: pup ratio	0.12	0.18	$< 0.01$
Number of embryos per dam	$11 \pm 2$	$9 \pm 1$	0.11
Rate of resorbed embryos (%)	7	24	<b>0.04</b>

**Table 1:** Fetal characteristics (Data is presented as  $\pm$  Standard Deviation).

### Placental genetic expression analysis

Mapping quality of the 24 RNA samples submitted was excellent. 1374 user IDs are unambiguously mapped to 1374 unique entrezgene IDs and 35 user IDs could not be mapped to any entrezgene ID. The GO Slim summary is based upon the 1374 unique entrezgene IDs. Among 1374 unique entrezgene IDs, 1233 IDs are annotated to the selected functional categories and also in the reference list, which are used for the

enrichment analysis. (See supplemental data-Figure 1). The principle component analysis comparing differentially expressed genes globally cluster between the hyperglycemic and euglycemia placentas at embryonic day 17.5 as shown in Figure 3.

Gene ontology (GO) enrichment analysis was performed to identify sets of DEGs overrepresented in this dataset. Enriched sets are categorized into biological process, cellular component, and molecular function. A total of 927 terms were significantly enriched in the biological process category, 126 in the cellular component category, and 141 in the molecular function category. Figure 4 shows the distribution of genes in each relevant biologic, cellular and molecular function category.

The top five most highly enriched GO terms for each category are listed in Tables 2-4. In the *biological processes*, among the top differentiated terms are regulation of chemo taxis, second messenger-mediated signaling, ossification, negative regulation of cell development and positive regulation of vascular development. In the *cellular components*, the top terms are related to the extracellular matrix, apical part of cell, external side of the plasma membrane, apical plasma membrane and collagen containing extracellular matrix. Finally, the top terms for *molecular function* included receptor regulator activity, receptor ligand activity, metal ion trans membrane transporter activity, symporter activity and channel activity. Based on the five most highly enriched terms, of the biological processes and cellular components, we performed histology relevant to vascular structure, development and function. A complete list of all genes that were differentially expressed between hyperglycemic exposed placentas and euglycemic exposed placentas can be found in the supplemental file links. Additional heat maps that demonstrate differential expression related to ossification, angiogenesis, and endothelial apoptosis between hyperglycemia exposed placentas and euglycemia exposed placentas are shown in Supplemental Figures 2-5.

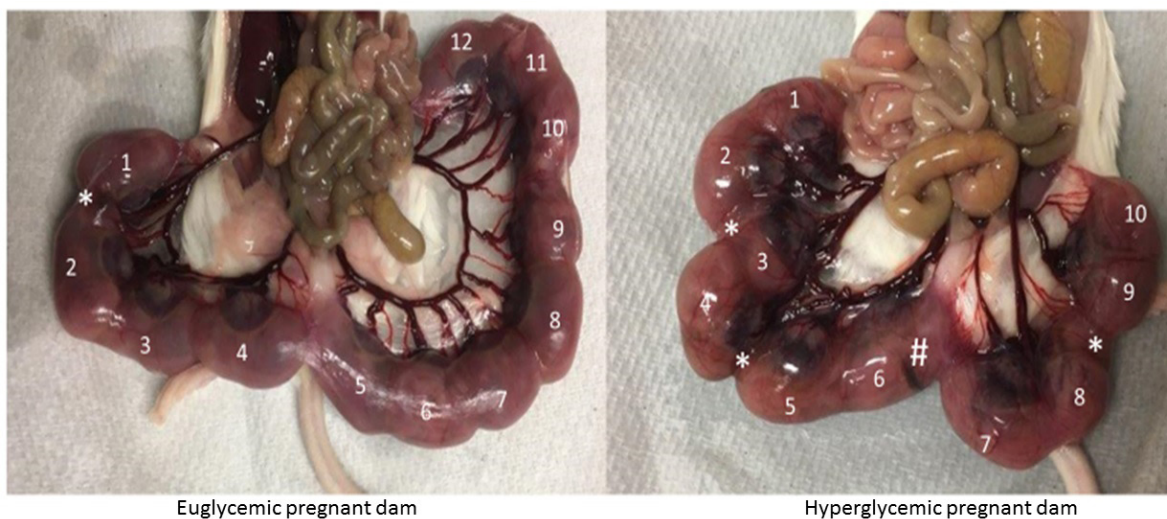


**Figure 2:** Hyperglycemia pregnancies result in higher rates of embryonic demise. A) Pregnancy of euglycemic dam at Embryonic day 17.5 (E17.5) with 12 fetuses (numbered counterclockwise each fetal placental unit). One resorbed embryo is noted at the location marked by (\*). B) Representative hyperglycemic pregnancy with 10 fetuses. Three resorbed embryos are marked by (\*), and a necrotic umbilical vessel can be seen marked by (#).

A. Biological process

Description	Number of genes Up	Number of genes Down
<b>Regulation of chemotaxis</b>	13	26
<b>Second-messenger-mediated Signaling</b>	24	35
<b>Ossification</b>	28	26
<b>Negative regulation of cell development</b>	18	34
<b>Positive regulation of vasculature development</b>	14	21

B. Cellular component

Description	Number of genes Up	Number of genes Down
<b>Extracellular matrix</b>	23	40
<b>Apical part of cell</b>	26	29
<b>External side of plasma membrane</b>	18	41
<b>Apical plasma membrane</b>	23	25
<b>Collagen-containing extracellular matrix</b>	15	28

C. Molecular function

Description	Number of genes Up	Number of genes Down
<b>Receptor regulator activity</b>	27	39
<b>Receptor ligand activity</b>	26	34
<b>Metal ion transmembrane transporter activity</b>	28	27
<b>Symporter activity</b>	20	8
<b>Channel activity</b>	28	26

**Table 2 (A-C):** Functional enrichment analysis. List of the top five significantly enriched elements.

Gene ontology (GO) enrichment analysis was performed to identify sets of DEGs overrepresented in this dataset. Enriched sets are categorized into biological process, cellular component, and molecular function. The top 5 most highly enriched GO terms for each category represent hyperglycemia placentas compared to euglycemia  $P < 0.001$  for all categories using  $FDR < 0.05$ . A total of 927 terms were significantly enriched in the biological process category, 126 in the cellular component category, and 141 in the molecular function category.

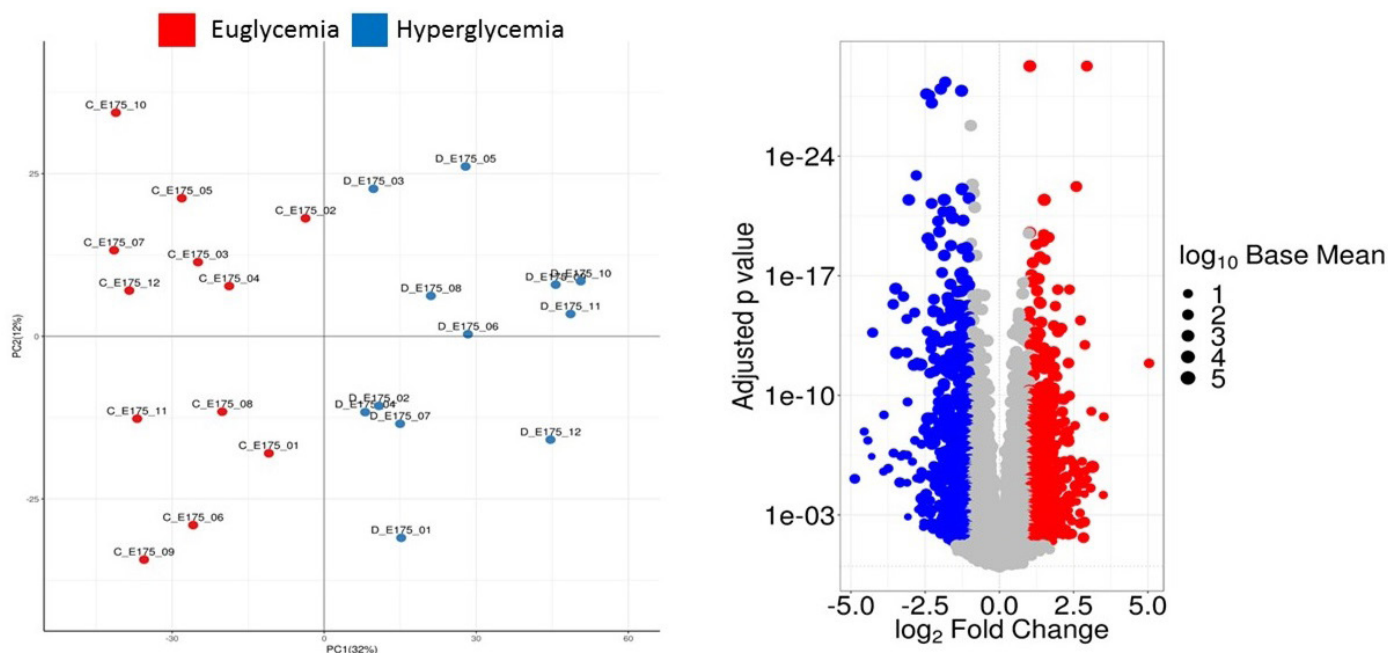


**Figure 3:** RNA sequencing demonstrates clear separation and clustering of differentially expressed genes by condition. A. Principle component analysis demonstrates clustering of gene expression by group Hyperglycemia (D) versus Euglycemia (C). B. Logarithmic fold change of genes differentially expressed in hyperglycemic placentas compared to euglycemic placentas.

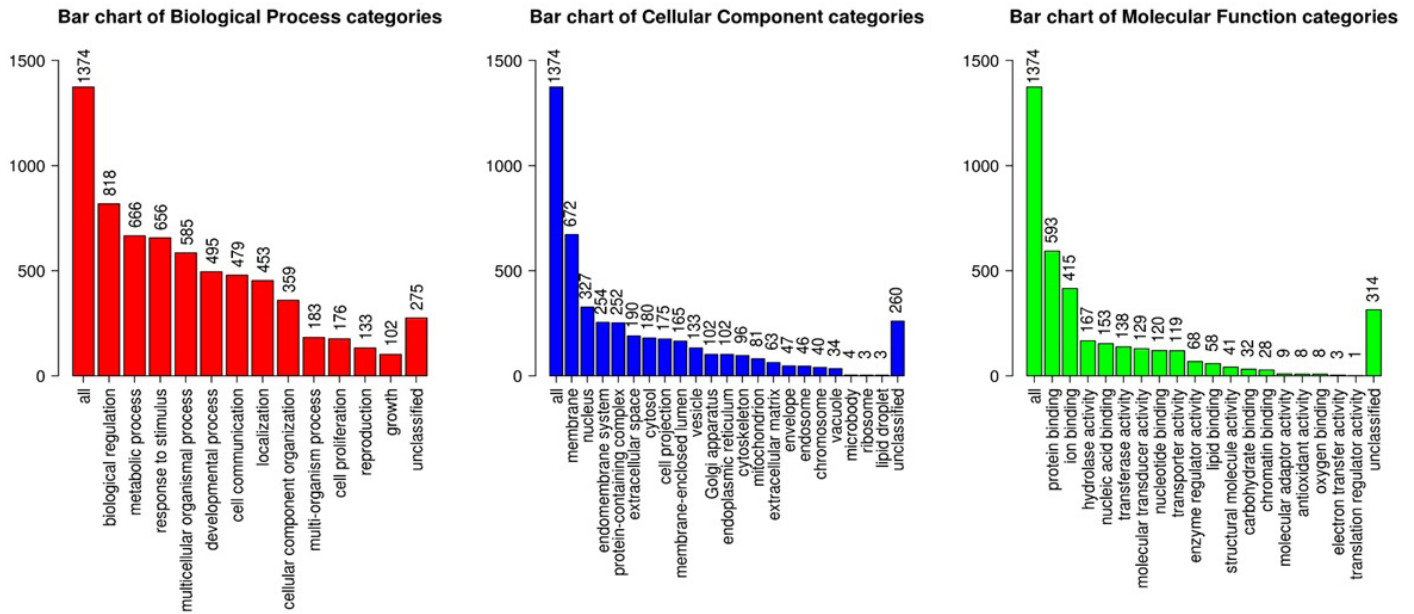


**Figure 4:** Number of genes in each category that correspond to biological process, cellular process and molecular function. The distribution of genes in each relevant biologic, cellular and molecular function category that demonstrated differential expression when comparing hyperglycemia to euglycemia placentas at embryonic day 17.5.

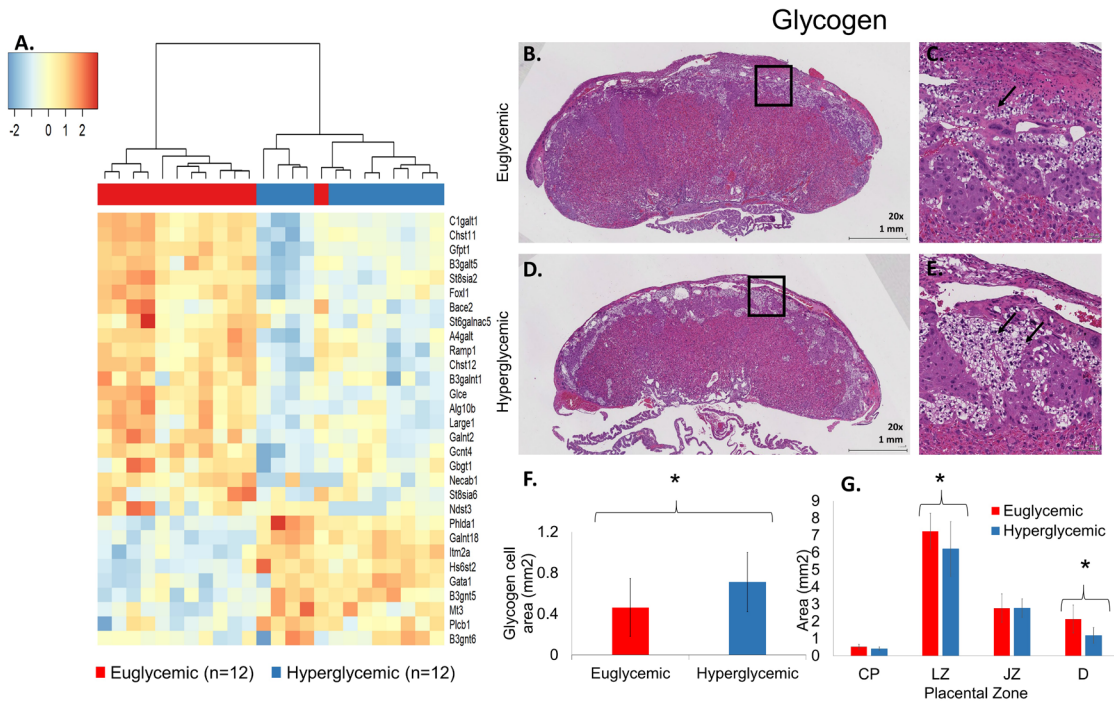


**Figure 5:** Maternal hyperglycemia causes differentially expressed genes in glycoprotein biosynthetic process and is associated with increased glycogen content in the labyrinth zone of the placenta.

**A).** Compared to euglycemic exposed placentas, hyperglycemic exposed placentas demonstrate decreased mRNA expression in *C1galt1*, *Chst11*, *Gfpt1*, *B3galt5*, *St8sia2*, *Foxl1*, *Bace2*, *St6galnac5*, *A4galt*, *Ramp1*, *Chst12*, *B3galnt1*, *Gfce*, *Alg10b*, *Large1*, *Galnt2*, *Gcnt4*, *Gbgt1*, *Necab1*, *St8sia6*, *Ndst3*, *Phlda1*, but increased expression of *Galnt18*, *Itih2a*, *Hs6st2*, *Gata1*, *B3gnt5*, *Mt3*, *Plcb1*, *B3gnt6*. ( $P$  value =  $< 10^{-7}$ , False discovery rate 0.05). **B).** Midline placental sections of euglycemia exposed placenta. **C.** Magnified junctional zone of euglycemia exposed placenta. **D.** Midline placental sections of hyperglycemia exposed placenta. **E.** Magnified junctional zone of hyperglycemia exposed placenta. Increased pockets of glycogen are clearly visible in the hyperglycemic sample. **F)** Glycogen cell area in euglycemic vs. hyperglycemic placental junctional zones ( $0.71 \pm 0.29 \text{ mm}^2$  vs.  $0.46 \pm 0.28 \text{ mm}^2$ ,  $p = 0.024$ ). **G)** Areas of zones in euglycemic vs. hyperglycemic placentas. \* =  $p < 0.05$ . Bars shown as means  $\pm$  standard deviation. Abbreviations: CP=chorionic plate, JZ=junctional zone, LZ=labyrinth zone, D=decidua.

Maternal hyperglycemia causes differentially expressed genes in glycoprotein biosynthetic process and is associated with increased glycogen content in the labyrinth zone of the placenta. Compared to euglycemic exposed placentas, hyperglycemic exposed placentas demonstrate decreased mRNA expression in *C1galt1*, *Chst11*, *Gfpt1*, *B3galt5*, *St8sia2*, *Foxl1*, *Bace2*, *St6galnac5*, *A4galt*, *Ramp1*, *Chst12*, *B3galnt1*, *Glce*, *Alg10b*, *LARGE1*, *Galnt2*, *Gcnt4*, *Gbgt1*, *Necab1*, *St8sia6*, *Ndst3*, *Phlda1*, but increased expression of *Galnt18*, *Itm2a*, *Hs6st2*, *Gata1*, *B3gnt5*, *Mt3*, *Plcb1*, *B3gnt6*. This correlated with increased glycogen content in the setting of hyperglycemia but decreased surface area in the labyrinth zone and the maternal decidua of the placenta as shown in Figure 5.

Maternal hyperglycemia causes differentially expressed genes in extracellular matrix organization and is associated with decreased collagen deposition in the chorionic plate and the junctional zone. Compared to euglycemic exposed placentas, hyperglycemic exposed placentas demonstrate decreased mRNA expression in *Fn1*, *Colgalt1*, *Itgb3*, *Tnfrsf1b*, *Pdgfra*, *Smad3*, *Vhl*, *Fbln1*, *Plod1*, *Aplp1*, *Foxf2*, *Focx2*, *Sh3pxd2b*, *Mmp9*, *Dmp1*, *Tnfrsf11b*, *Antxr1Grem1*, *Cma1*, *Otol1*, *Tnf*, *Npnt*, *Colq*, *Ctss*, and *Mmp13*. However, hyperglycemia exposed placentas demonstrate an increase in *Ramp2*, *Sfrp2*, *Col11a1*, *Mdap4*, *Col4a6*, *Col23a1*, *Col13a1*, *Col4a5* and *Vit*. These genetic differences correlated with a reduction in collagen in the fetal vessels and the junctional zone shown in Figure 6.

Maternal hyperglycemia causes differential expression of genes of endothelial cell proliferation and is associated with increased proliferation in the junctional zone and labyrinth zones of the placenta. Compared to euglycemic exposed placentas, hyperglycemic exposed placentas demonstrate decreased mRNA expression in *Fgfr1*, *Htr2b*, *Itgb3*, *Akt3*, *Prkd1*, *Il10*, *Fgf2*, *Ang*, and *ApoH* in 10/12 placenta samples. However, hyperglycemia exposed placentas demonstrated increased *Jun*, *Nr4a1*, *Ager*, *Apela*, *Ppp1r16b*, *Aplnr*, *Lrg1*. The genetic variation between hyperglycemic exposed placenta and euglycemic exposed placenta led to increase of Ki67 in the junctional and labyrinth zones shown in Figure 7.

Additionally, maternal hyperglycemia caused differential expression of genes in the positive regulation of the apoptosis. Compared to euglycemic exposed placentas, hyperglycemic exposed placentas demonstrate decreased mRNA expression of *Bcl211*, *Sfrp1*, *Moap1*, *Inhba*, *Siglec1*, *Mmp9*, *Inhbb*, *Smad3*, *Timp3*, *Ret*, *Ctsc* and *Il19*. However, *Fas*, *Trp63*, *Atf3*, *Mal*, *Rpl26*, *Nkx3-1* have a higher expression in hyperglycemia exposed placentas. The genetic variation between hyperglycemic exposed placenta and euglycemic exposed placenta led to increase of Caspase 3- a marker for apoptosis in the labyrinth zones shown in Figure 8.

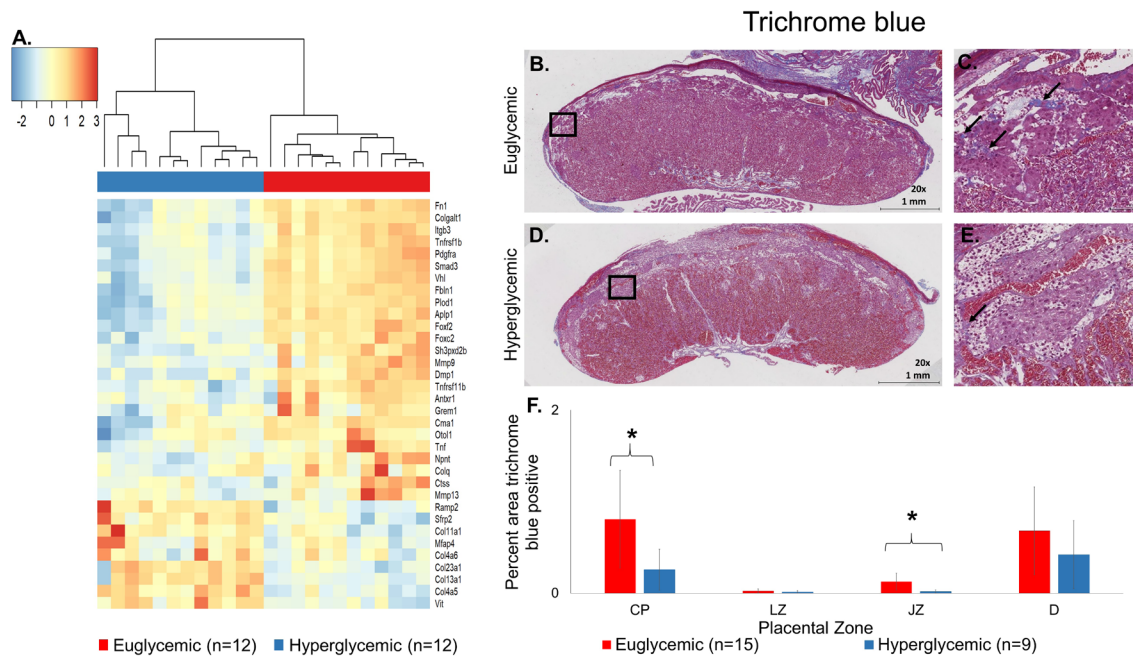


**Figure 6:** Maternal hyperglycemia causes differentially expressed genes in extracellular matrix organization and is associated with decreased collagen deposition in the chorionic plate and the junctional zone. **A.** Compared to euglycemic exposed placentas, hyperglycemic exposed placentas demonstrate decreased mRNA expression in *Fn1*, *Colgalt1*, *Itgb3*, *Tnfrsf1b*, *Pdgfra*, *Smad3*, *Vhl*, *Fbln1*, *Plod1*, *Aplp1*, *Foxf2*, *Focx2*, *Sh3pxd2b*, *Mmp9*, *Dmp1*, *Tnfrsf11b*, *Antxr1Grem1*, *Cma1*, *Otol1*, *Tnf*, *Npnt*, *Colq*, *Ctss*, and *Mmp13*. However, hyperglycemia exposed placentas demonstrate an increase in *Ramp2*, *Sfrp2*, *Col11a1*, *Mdap4*, *Col4a6*, *Col23a1*, *Col13a1*, *Col4a5* and *Vit*. ( $P$  value  $< 10^{-7}$ , False discovery rate 0.05). **B.** Midline placental sections of euglycemia exposed placenta. **C.** Magnified junctional zone of euglycemia exposed placenta. **D.** Midline placental sections of hyperglycemia exposed placenta. **E.** Magnified junctional zone of hyperglycemia exposed placenta. Arrows pointing to positive blue staining. Representative placentas stained with Masson's trichrome blue. **F.** Collagen deposition per zone measured by percent trichrome blue staining. Areas of zones in euglycemic vs. hyperglycemic placentas.  $* = p < 0.05$ . Bars shown as means  $\pm$  standard deviation. Abbreviations: CP=chorionic plate, JZ=junctional zone, LZ=labyrinth zone, D=decidua.

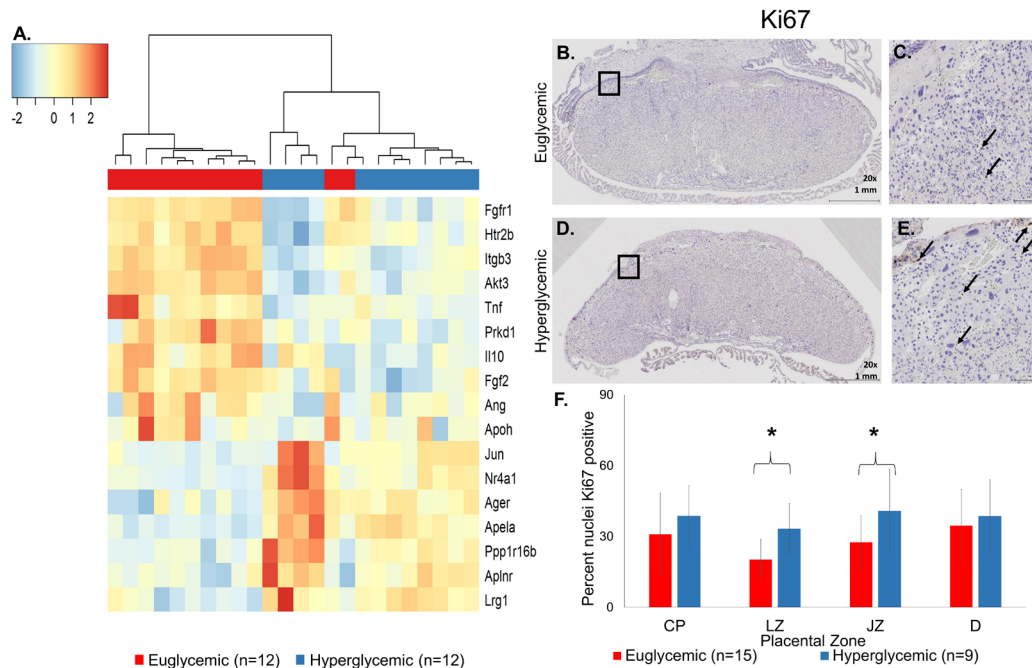


**Figure 7:** Maternal hyperglycemia causes differential expression of genes of endothelial cell proliferation and is associated with increased proliferation in the junctional zone and labyrinth zones of the placenta. **A).** Compared to euglycemic exposed placentas, hyperglycemic exposed placentas demonstrate decreased mRNA expression in *Fgfr1*, *Htr2b*, *Itgb3*, *Akt3*, *Prkd1*, *Il10*, *Fgf2*, *Ang*, and *Apoh* in 10/12 placenta samples. However, hyperglycemia exposed placentas demonstrated increased *Jun*, *Nr4a1*, *Ager*, *Apela*, *Ppp1r16b*, *Aplnr*, *Lrg1*. ( $P$  value  $\leq 10^{-7}$ , False discovery rate 0.05). **B).** Midline placental sections of euglycemia exposed placenta. **C).** Magnified junctional and labyrinth zones of euglycemia exposed placenta. **D).** Midline placental sections of hyperglycemia exposed placenta. **E).** Magnified junctional zone and labyrinth zone of hyperglycemia exposed placenta. Arrows pointing to positive immunostaining of Ki67. **F).** Proliferation per zone measured by percent positive nuclear Ki67 staining of zones in euglycemic vs. hyperglycemic placentas.  $* = p < 0.05$ . Bars shown as means  $\pm$  standard deviation. Abbreviations: CP=chorionic plate, JZ=junctional zone, LZ=labyrinth zone, D=decidua.

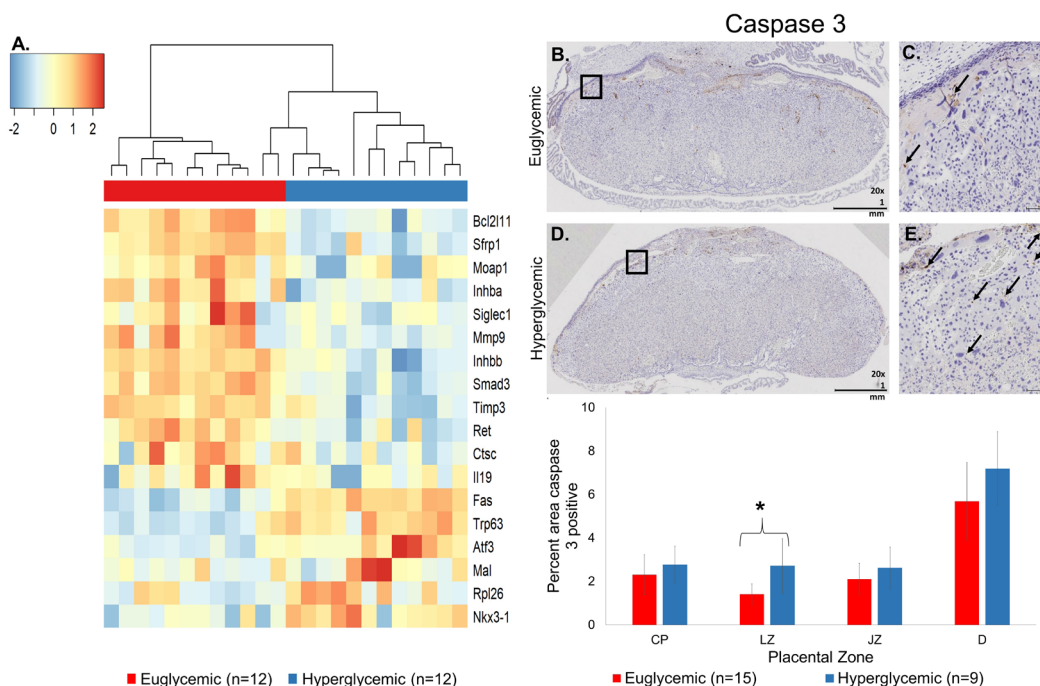


**Figure 8:** Maternal hyperglycemia causes differential expression of genes in the positive regulation of apoptotic signaling pathway. **A).** Compared to euglycemic exposed placentas, hyperglycemic exposed placentas demonstrate decreased mRNA expression of *Bcl2l11*, *Sfrp1*, *Moap1*, *Inhba*, *Siglec1*, *Mmp9*, *Inhbb*, *Smad3*, *Timp3*, *Ret*, *Ctsc* and *Il19*. However, *Fas*, *Trp63*, *Atf3*, *Mal*, *Rpl26*, *Nkx3-1* have a higher expression in hyperglycemia exposed placentas ( $P$  value  $\leq 10^{-7}$ , False discovery rate 0.05). **B).** Midline placental sections of euglycemia exposed placenta. **C).** Magnified junctional and labyrinth zones of euglycemia exposed placenta. **D).** Midline placental sections of hyperglycemia exposed placenta. **E).** Magnified junctional zone and labyrinth zone of hyperglycemia exposed placenta. Arrows pointing to positive immunostaining of Caspase 3. **F).** Apoptosis per zone measured by percent area caspase 3 positive.  $* = p < 0.05$ . Bars shown as means  $\pm$  standard deviation. Magnified views of LZ. Bars shown as means  $\pm$  standard deviation. Abbreviations: CP=chorionic plate, JZ=junctional zone, LZ=labyrinth zone, D=decidua.

---

## Comment

### Principal findings

We have shown that pregestational maternal hyperglycemia in mice causes widespread disruption in gene expression. Many of the gene ontology (GO) terms in the biological function category enriched in this set of DEGs are important to angiogenesis, vascular development and morphogenesis of a branching structure. This widespread disruption in gene expression are associated with higher rates of embryonic demise and abnormal placental morphology including increased glycogen content decreased collagen deposition, and increased cellular apoptosis and proliferation. This study uses an unbiased genome wide RNA sequencing platform to detect differential expression between hyperglycemia and euglycemia in animals. RNA sequencing is a relatively new technology that has enabled us to perform high throughput screening. In contrast to Yu and colleagues who utilized a microarray with prespecified 118 genes of which 75 were unclassified? This approach opens up the opportunity to identify candidate genes differentially expressed in the setting of maternal hyperglycemia, not previously known to be important in vascular development or function.

### Results

Many of the differentially expressed genes are plausible contributors to placental dysfunction in maternal diabetes and relate directly to clinically observed phenotypes, providing potential therapeutic targets for intervention. *Prom1* and *Pde4d* are important in the angiogenesis pathway and had previously been shown to be critical in implantation and early embryonic development [24,25]. Abnormal expression of *Prom1* could lead to abnormal interaction of the cytotrophoblast to the maternal spiral arteries in the decidua resulting in placenta dysfunction. Importantly other genes detrimental to endothelial function by increasing oxidative stress were significantly upregulated. *Cyp11a1*, a gene that encodes for cytochrome P450, was significantly overexpressed in our diabetic placentas and demonstrated a 32 fold increase in gene expression. This gene encodes for a cytochrome P450 protein which contributes to the nitric oxide (NO) system of blood pressure regulation [25]. Dr Yu also reported increased expression in *Cyp11a1* but to a lower degree (1.4 fold) [22]. Direct embryonic toxicity can be mediated via the *Pax1* is a homeobox gene. Mouse models with a mutation in *Pax1* have altered glycosylation patterns associated with embryologic malformations and embryonic demise [26]. *Esx1* is another homeobox transcription factor gene that results in the development of larger than normal LZ with decreased vascular density [27], similar to the changes in the LZ noted in this study. Increased levels of sFlt-1 in murine placentas appears to cause decreased differentiation of spongiotrophoblast cells into glycogen cells [13], though increased glycogen deposition has also been observed in human placentas complicated by all forms of diabetes [14].

*Nrn1* previously known to be important in neuron development has also been shown to be important for angiogenesis [26]. *Foxl2* has been shown to be crucial on the response to hypoxia [27]. *Ccr5* promotes vascular smooth muscle cell proliferation [28]. *Sema6d* is critical to cardiomyocyte and endocardial cushion development

[29]. However, the large number and variety of DEGs and enriched pathways support the notion that diabetes has widespread effects on placental development, and the placental dysfunction that manifest as embryonic demise and maternal preeclampsia in the setting of diabetes is not isolated to one pathway or gene.

### Clinical Implications

Predisposition to placental dysfunction begins to be established early in the first trimester [30]. Failure to seek medical care in this critical time frame may lead to pregnancies of patients with T1DM being exposed to severe hyperglycemia around the time of placenta development.

### Research Implications

Our approach to gene discovery is novel in that we applied an unbiased genome wide mRNA expression profile and correlated candidate gene pathways with placental histology. Moreover, using this approach enables us to characterize differential expression in other organ systems as well. In surveying our data, we have a vast reservoir of gene pathways differentially expressed important in renal function, neurodevelopmental pathways, cardiac development, embryonic development and metabolic function (See supplemental KEGG Gene Enrichment Report). Future research will focus on other types of pregestational diabetes and their disruption of the gene expression of vascular important genes. Additionally, we will investigate epigenetic modifications that influence differences in gene expression between hyperglycemia and euglycemia exposed placentas such as DNA methylation. This will enable us to understand the underlying mechanisms that lead to abnormal gene expression.

### Strengths and Limitations

The clinical relevance is a significant strength to our study. In human disease T1DM incurs a greater risk of placenta dysfunction. Compared to T2DM and GDM, mothers with T1DM have higher incidences of embryopathy, fetal growth restriction, stillbirth, maternal preeclampsia and small vessel disease [28]. They are also more likely to have poor glycemic control throughout pregnancy (evidenced by higher hemoglobin A1C) making earlier delivery for suboptimal glycemia control and preeclampsia more likely [2,4]. Thus, our T1DM model captures the cohort of patients with the disproportionate burden of adverse pregnancy outcomes. In considering potential limitations, we would like to address that our results must be interpreted in the context of a T1DM model of untreated pregestational diabetes. Although T1DM represents a smaller fraction of all pregnancies affected diabetes, it carries a disproportionately higher burden of adverse pregnancy outcomes compared to other T2DM or GDM [5]. Additionally, STZ was administered intraperitoneally. STZ gains entry into the beta- islet cell via GLUT-2 receptors in the pancreas [9]. STZ may have off target toxic effects to intraabdominal organs such as the ovaries. We did not test the effects of STZ to the ovaries or uterus that could potentially affect placental development. However, this is unlikely given the fact that GLUT-2 receptors are concentrated to the liver and the pancreas [9]. The short half-life of STZ (48 hours), coupled with the fact that the females were mated two weeks

after confirmation of hyperglycemia make ovarian toxicity from STZ at the time of conception unlikely [29]. Lastly, we initially hypothesized that the dams would demonstrate hypertension. Although they were not hypertensive, they had a trend in elevated urine albumin to creatinine ratio. It is possible that the hyperglycemic dams did not demonstrate hypertension due to severe hypovolemia in the setting of untreated hyperglycemia. Other studies with Non-obese diabetic mice also noted paradoxically hypotension in the setting of pregestational diabetes and pregnancy [30,31].

## Conclusion

Maternal diabetes causes widespread disruption in multiple cellular processes important for normal vascular development and sets the platform for placenta dysfunction. There was a higher rate of resorptions or spontaneous miscarriages in the pregnancies of hyperglycemic dams. Pregestational diabetes results in significant changes in placental morphology, including increased weight, decreased labyrinth zone size, and increased glycogen deposition in the junctional zone. Increased apoptosis and proliferation in the labyrinth zone resulted in increased cell turnover and vascular dysfunction. In a mouse model of pregestational type 1 diabetes, whole transcriptome sequencing can illuminate mechanisms of placental dysfunction that cause diabetes-mediated dysfunction. These genetic insights can identify potential genetic pathway targets for therapy or prevention.

## Highlights

Maternal diabetes causes abnormal gene expression in placentas leading to abnormal placenta structure and function.

**Condensation:** Maternal diabetes causes widespread disruption in multiple cellular processes important for normal vascular development and sets the platform for placenta dysfunction.

The underlying mechanisms of placental dysfunction in setting of pregestational diabetes are not well understood. Maternal diabetes causes genome wide differential gene expression of multiple cellular processes and results in significant changes in placental morphology which set the stage for complications observed in maternal type 1 diabetes mellitus. Whole transcriptome sequencing illuminates genetic associations of placental dysfunction.

## Acknowledgements

This study was supported by the National Institutes of Health Grant by the **NHLBI 5 K01 HL140278-02**.

This paper was presented at the 40<sup>th</sup> Annual Pregnancy Meeting hosted by the Society of Maternal Fetal Medicine, February 3-8, 2020 in Grapevine, TX.

A special thanks to Building Interdisciplinary Careers in Women's Health Working Group for editorial support, 2525 West End Avenue, Nashville, TN 37232

A special thanks to Wonder, P DRAKE, MD, for lending editorial support, Division of Infectious Diseases, Department of Medicine,

Vanderbilt University Medical Center, 1211 Medical Center Dr, Nashville, TN 37232

A special thanks to the Translational Pathology Shared Resource for sectioning and staining of placenta slides. We acknowledge the Translational Pathology Shared Resource supported by NCI/NIH Cancer Center Support Grant 5P30 CA68485-19 and the Vanderbilt Mouse Metabolic Phenotyping Center Grant 2 U24 DK059637-16, Kelli BOYD, DVM, PhD, DACVP, Nashville, TN, United States, Department of Pathology, Microbiology and Immunology, Translational Pathology Shared Resource, Vanderbilt University Medical Center, 1211 Medical Center Dr, Nashville, TN 37232.

A special thanks for blood pressure assessments to, Lin ZHONG, M.D. PhD, Nashville, TN, United States, Department of Medicine, Vanderbilt University Medical Center, 1211 Medical Center Dr, Nashville, TN 37232.

A special thanks to Digital Histology Shared Resource for acquisition of images and imaging software support, Joseph Roland, PhD, Vanderbilt University Medical Center 10425-C MRB IV 2213 Garland Ave, Nashville, TN 37232-0443.

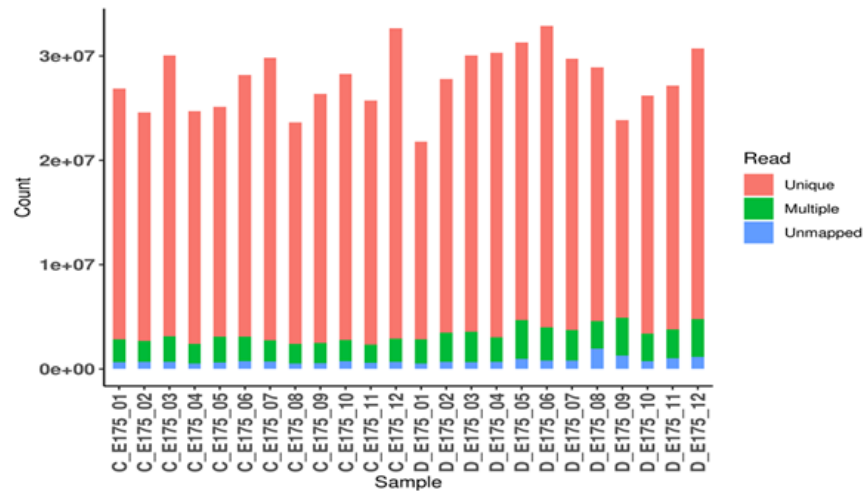
## References

1. Alexopoulos AS, Blair R, Peters AL. Management of Preexisting Diabetes in Pregnancy: A Review. *Jama*. 2019; 321: 1811-1819.
2. Stogianni A, Lena Lendahls, Mona Landin-Olsson, et al. Obstetric and perinatal outcomes in pregnancies complicated by diabetes, and control pregnancies, in Kronoberg, Sweden. *BMC Pregnancy Childbirth*. 2019; 19: 159.
3. Persson M, Norman M, Hanson U. Obstetric and perinatal outcomes in type 1 diabetic pregnancies: A large, population-based study. *Diabetes Care*. 2009; 32: 2005-2009.
4. Knight KM, Thornburg LL, Pressman EK. Pregnancy outcomes in type 2 diabetic patients as compared with type 1 diabetic patients and nondiabetic controls. *J Reprod Med*. 2012; 57: 397-404.
5. Hemberger M, Hanna CW, Dean W. Mechanisms of early placental development in mouse and humans. *Nat Rev Genet*. 2020; 21: 27-43.
6. Rossant J, Cross JC. Placental development: lessons from mouse mutants. *Nat Rev Genet*. 2001; 2: 538-548.
7. Anjali A Sarkar, Samer J Nuwayhid, Thomas Maynard, et al. Hectd1 is required for development of the junctional zone of the placenta. *Dev Biol*. 2014; 392: 368-380.
8. Szkudelski T. The mechanism of alloxan and streptozotocin action in B cells of the rat pancreas. *Physiol Res*. 2001; 50: 537-546.
9. Amin Al-Awar, Krisztina Kupai, Médea Veszélka, et al. Experimental Diabetes Mellitus in Different Animal Models. *J Diabetes Res*. 2016; 9051426.

10. Murphy HR, Steel SA, Roland JM, et al. Obstetric and perinatal outcomes in pregnancies complicated by Type 1 and Type 2 diabetes: influences of glycaemic control, obesity and social disadvantage. *Diabet Med.* 2011; 28: 1060-1067.
11. Evers IM, de Valk HW, Visser GH. Risk of complications of pregnancy in women with type 1 diabetes: nationwide prospective study in the Netherlands. *BMJ.* 2004; 328: 915.
12. Parchem JG, Keizo Kanasaki, Megumi Kanasaki, et al. Loss of placental growth factor ameliorates maternal hypertension and preeclampsia in mice. *J Clin Invest.* 2018; 128: 5008-5017.
13. Radenković M, Stojanović M, Prostran M. Experimental diabetes induced by alloxan and streptozotocin: The current state of the art. *J Pharmacol Toxicol Methods.* 2016; 78: 13-31.
14. Clee SM, Attie AD. The genetic landscape of type 2 diabetes in mice. *Endocr Rev.* 2007; 28: 48-83.
15. Feng M, DiPetrillo K. Non-invasive blood pressure measurement in mice. *Methods Mol Biol.* 2009; 573: 45-55.
16. Kechin A, Uljana Boyarskikh, Alexander Kel, et al. CutPrimers: A New Tool for Accurate Cutting of Primers from Reads of Targeted Next Generation Sequencing. *J Comput Biol.* 2017; 24: 1138-1143.
17. Dobin A, Davis CA, Schlesinger F, et al. STAR: ultrafast universal RNA-seq aligner. *Bioinformatics.* 2013; 29: 15-21.
18. Liao Y, Smyth GK, Shi W. Feature Counts: an efficient general-purpose program for assigning sequence reads to genomic features. *Bioinformatics.* 2014; 30: 923-930.
19. Love MI, Huber W, Anders S. Moderated estimation of fold change and dispersion for RNA-seq data with DESeq2. *Genome Biol.* 2014; 15: 550.
20. Zhao S, Guo Y, Shenget Q, et al. Advanced heat map and clustering analysis using heatmap3. *Biomed Res Int.* 2014; 986048.
21. Wang J, Vasaikar S, Shi Z, et al. Web Gestalt 2017: a more comprehensive, powerful, flexible and interactive gene set enrichment analysis toolkit. *Nucleic Acids Res.* 2017; 45: W130-W137.
22. Yu Y, Singh U, Shi W, et al. Influence of murine maternal diabetes on placental morphology, gene expression, and function. *Arch Physiol Biochem.* 2008; 114: 99-110.
23. Leonard AK, Loughran EA, Klymenko Y, et al. Methods for the visualization and analysis of extracellular matrix protein structure and degradation. *Methods Cell Biol.* 2018; 143: 79-95.
24. Dowland SN, Madawala RJ, Poon CE, et al. Prominin-1 glycosylation changes throughout early pregnancy in uterine epithelial cells under the influence of maternal ovarian hormones. *Reprod Fertil Dev.* 2017; 29: 1194-1208.
25. Bartsch O, Bartlick B, Ivell R. Phosphodiesterase 4 inhibition synergizes with relaxin signaling to promote decidualization of human endometrial stromal cells. *J Clin Endocrinol Metab.* 2004; 89: 324-334.
26. Han D, Bo Qin, Guoqing Liu, et al. Characterization of neuritin as a novel angiogenic factor. *Biochem Biophys Res Commun.* 2011; 415: 608-612.
27. Ter Horst EN, Nynke E Hahn, Dirk Geerts, et al. p47phox-Dependent Reactive Oxygen Species Stimulate Nuclear Translocation of the FoxO1 Transcription Factor During Metabolic Inhibition in Cardiomyoblasts. *Cell Biochem Biophys.* 2018; 76: 401-410.
28. Lin CS, Hsieh PS, Hwang LL, et al. The CCL5/CCR5 Axis Promotes Vascular Smooth Muscle Cell Proliferation and Atherogenic Phenotype Switching. *Cell Physiol Biochem.* 2018; 47: 707-720.
29. Sun Q, Peng Y, Zhao Q, et al. SEMA6D regulates perinatal cardiomyocyte proliferation and maturation in mice. *Dev Biol.* 2019; 452: 1-7.
30. Burke SD, Barrette VF, David S, et al. Circulatory and renal consequences of pregnancy in diabetic NOD mice. *Placenta.* 2011; 32: 949-955.
31. Aasa KL, Kwong KK, Adams MA, et al. Analysis of maternal and fetal cardiovascular systems during hyperglycemic pregnancy in the nonobese diabetic mouse. *Biol Reprod.* 2013; 88: 151.

Parameter	Euglycemia (n=6)	Hyperglycemia (n=3)	P-value
Pregestational weight (g)	30.23 ± 1.6	29.64 ± 1.9	0.37
Blood glucose (mg/dL)	112 ± 24	473 ± 47	<0.01
Gestational weight gain (g)	6.31 ± 7.0	11.57 ± 2.5	0.37
Number of embryos	11 ± 2	9 ± 1	0.11
Rate of resorbed embryos (%)	7	24	0.04
Mean arterial pressure (mmHg)	95.9 ± 24.8	61.4 ± 9.8	0.0053
Urine albumin to creatinine ratio	61.4 ± 89.3	1242.3 ± 1126.8	0.0588

Supplemental Table 1: Maternal characteristics (Data is presented as ± Standard Deviation).



Supplemental Figure 1: Mapping quality 1374 user IDs are unambiguously mapped to 1374 unique entrezgene IDs and 35 user IDs cannot be mapped to any entrezgene ID. The GO Slim summary is based upon the 1374 unique entrezgene IDs. Among 1374 unique entrezgene IDs, 1233 IDs are annotated to the selected functional categories and also in the reference list, which are used for the enrichment analysis.

Reference list: all mapped entrezgene IDs from the selected platform genome. The reference list can be mapped to 68167 entrezgene IDs and 18986 IDs are annotated to the selected functional categories that are used as the reference for the enrichment analysis.

**A. Biological process**

Description	Number of genes Up	Number of genes Down
Regulation of chemotaxis	13	26
Second-messenger-mediated Signaling	24	35
Ossification	28	26
Negative regulation of cell development	18	34
Positive regulation of vasculature development	14	21

**B. Cellular component**

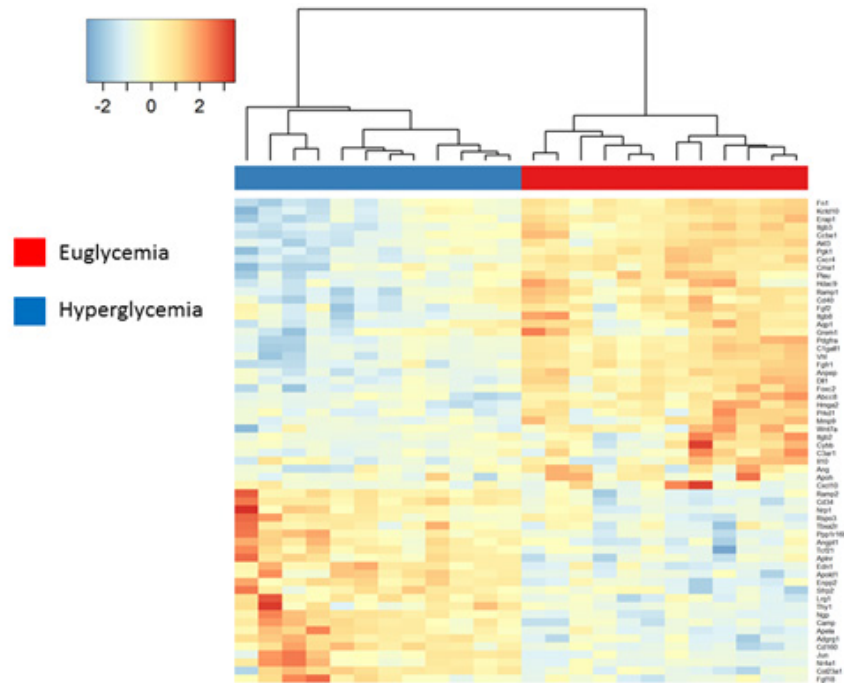
Description	Number of genes Up	Number of genes Down
Extracellular matrix	23	40
Apical part of cell	26	29
External side of plasma membrane	18	41
Apical plasma membrane	23	25
Collagen-containing extracellular matrix	15	28

**C. Molecular function**

Description	Number of genes Up	Number of genes Down
Receptor regulator activity	27	39
Receptor ligand activity	26	34
Metal ion transmembrane transporter activity	28	27
Symporter activity	20	8
Channel activity	28	26

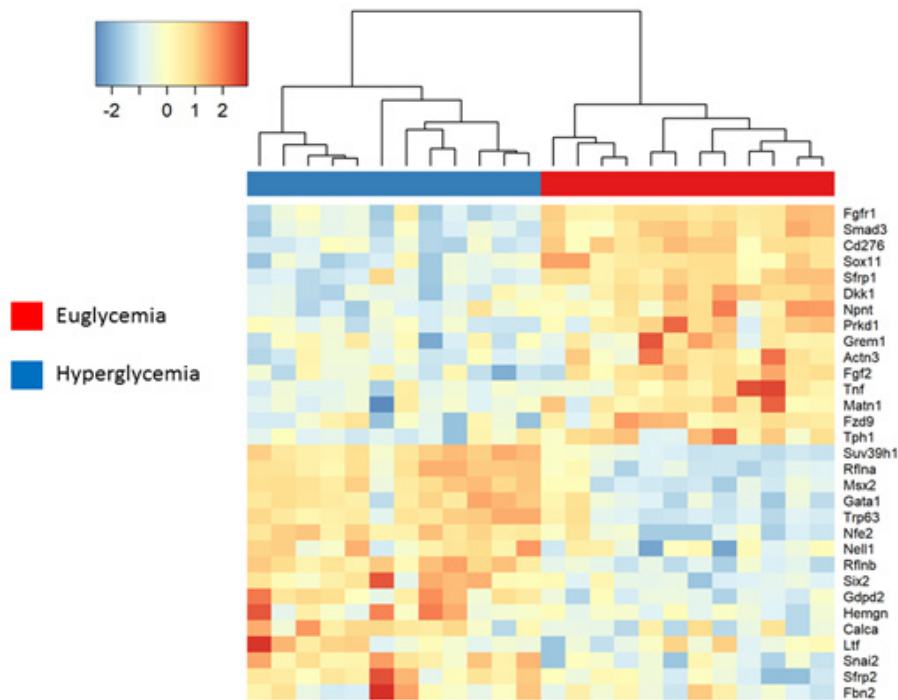
Supplemental Table 2 (A-C): Functional enrichment analysis. List of the top five significantly enriched elements.

Gene ontology (GO) enrichment analysis was performed to identify sets of DEGs overrepresented in this dataset. Enriched sets are categorized into biological process, cellular component, and molecular function. The top 5 most highly enriched GO terms for each category represent hyperglycemia placentas compared to euglycemia P<0.001 for all categories using FDR <0.05. A total of 927 terms were significantly enriched in the biological process category, 126 in the cellular component category, and 141 in the molecular function category.

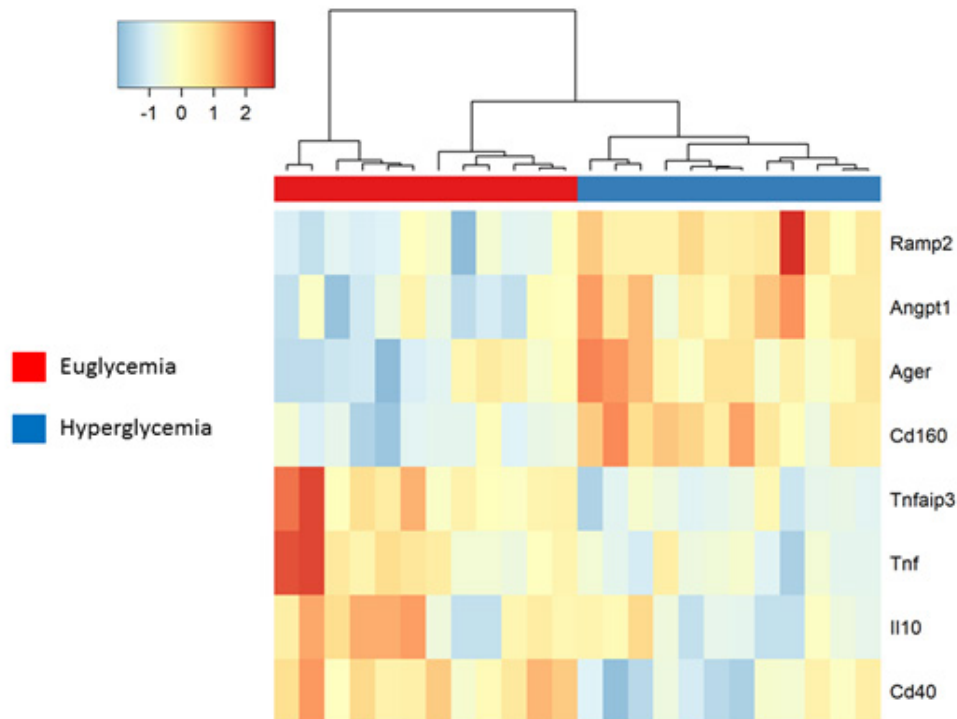


**Supplemental Figure 2:** Significantly differential expressed genes in angiogenesis.

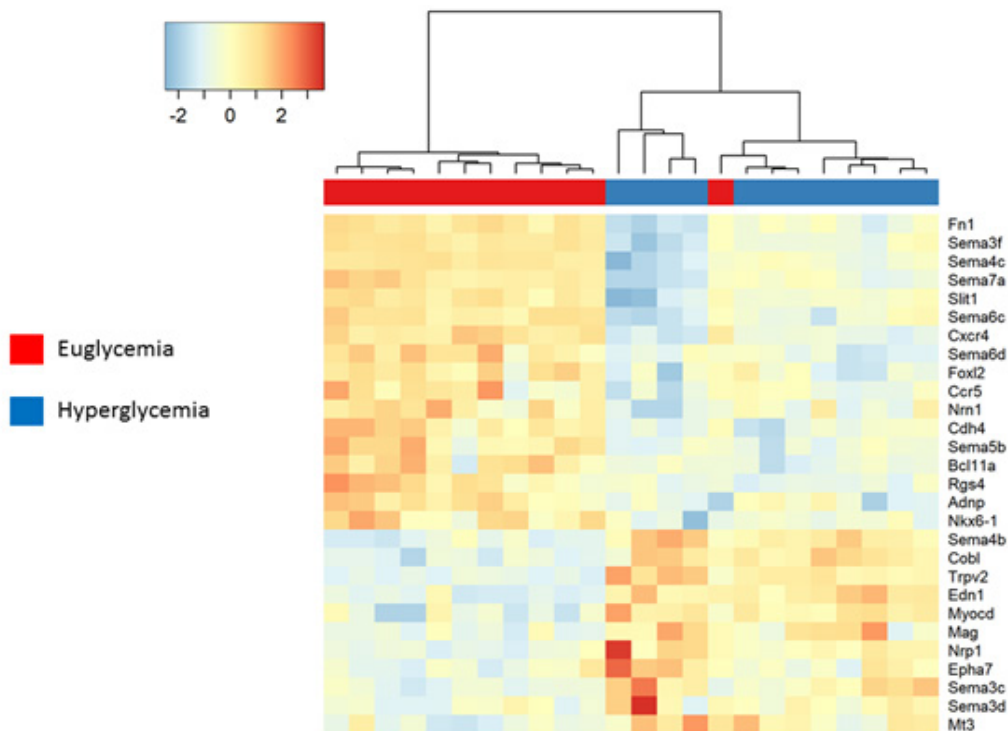
Compared to euglycemic exposed placentas, maternal hyperglycemic exposed placentas causes decreased mRNA expression of genes *Fn1*, *Kctd10*, *Erap1*, *Itgb3*, *Ccbe1*, *Akt3*, *Pgk1*, *Cxcr4*, *Cma1*, *Plau*, *Hdac9*, *Ramp1*, *Cd40*, *Fgf2*, *Itgb8*, *Aqp1*, *Grem1*, *Pdgfra*, *C1galt1*, *Vhl*, *Fgfr1*, *Anpep*, *Dll1*, *Foxc2*, *Abcc2*, *Hmga2*, *Prkd1*, *Mmp9*, *Wnt7a*, *Itgb2*, *Cybb*, *C3ar1*, *Il10*, *Ang*, and *ApoH*. However, hyperglycemic exposed placentas demonstrate increased expression of *Cxcl10*, *Ramp2*, *Cd34*, *Nrp1*, *Rspo3*, *Tbxa2r*, *Ppp1r16b*, *Angpf1*, *Tcf21*, *Aplnr*, *Edn1*, *Apold1*, *Enpp2*, *Sfrp2*, *lrg1*, *Thy1*, *Ngp*, *Camp*, *Apela*, *Adgrg1*, *Cd160*, *Jun*, *Nr4a1*, *Col23a1*, *Fgf18* ( $P$  value= $<10^{-7}$ , False discovery rate 0.05).



**Supplemental Figure 3:** Maternal hyperglycemia causes differential expression of genes associated with ossification pathway. Compared to euglycemic exposed placentas, maternal hyperglycemia causes decreased mRNA expression of genes *Fgfr1*, *Smad3*, *Cd276*, *Sox11*, *Sfrp1*, *Dkk1*, *Npnt*, *Prkd1*, *Grem1*, *Actn3*, *Fgf2*, *Tnf*, *Matn1*, *Fzd9* and *Tph1*. Conversely, maternal diabetes causes upregulation of *Suv39h1*, *Rflna*, *Mx2*, *Gata1*, *Trp63*, *Nfe2*, *Nell1*, *Rflnb*, *Six2*, *Gdpd2*, *Hemgn*, *Calca*, *Ltf*, *Snai2*, *Sfrp2* and *Fbn2*. ( $P$  value= $<10^{-7}$ , False discovery rate 0.05).



**Supplemental Figure 4:** Maternal hyperglycemia causes differential expression of genes associated with genes in the endothelial cell apoptotic process. Compared to euglycemic exposed placentas, maternal hyperglycemia causes increased mRNA expression of *Ramp2*, *Angpt1*, *Ager*, and *Cd160* are upregulated. Conversely *Tnfaip3*, *Tnf*, *Il10* and *Cd40* are downregulated in hyperglycemic placentas compared to euglycemic placentas ( $P$  value= $<10^{-7}$ , False discovery rate 0.05).



**Supplemental Figure 5:** Maternal hyperglycemia causes differential expressed genes in developmental cell growth. Compared to euglycemic exposed placentas, maternal hyperglycemia causes decreased mRNA expression *Fn1*, *Sema3f*, *Sema7a*, *Slit1*, *Sema6c*, *Cxcr4*, *Sema6d*, *Foxl2*, *Ccr5*, *Nrn1*, *Cdh4*, *Sema5b*, *Bcl11a*, *Rgs4*, *Adnp*, *Nkx6-1*. However, hyperglycemia exposed placentas demonstrate a higher expression of *Sema4b*, *Cobl*, *Trpv2*, *Edn1*, *Myocd*, *Mag*, and *Nrp1*. ( $P$  value= $<10^{-7}$ , False discovery rate 0.05).

---

## Weblinks to Gene Ontology Data

### Supplemental weblink-1 Biological process

file:///C:/Users/listerrl/AppData/Local/Temp/Rar\$EXa0.402/20190403\_rnaseq\_2499\_lister\_mouse\_placenta\_cutadapt/report/result/rnaseq\_Diabetic\_E175/enrichment\_results\_E175\_D\_vs\_C\_geneontology\_Biological\_Process.txt.html

### Supplemental weblink-2 Cellular component

file:///C:/Users/listerrl/AppData/Local/Temp/Rar\$EXa0.434/20190403\_rnaseq\_2499\_lister\_mouse\_placenta\_cutadapt/report/result/rnaseq\_Diabetic\_E175/enrichment\_results\_E175\_D\_vs\_C\_geneontology\_Cellular\_Component.txt.html

### Supplemental weblink-3 Molecular Function

file:///C:/Users/listerrl/AppData/Local/Temp/Rar\$EXa0.173/20190403\_rnaseq\_2499\_lister\_mouse\_placenta\_cutadapt/report/result/rnaseq\_Diabetic\_E175/enrichment\_results\_E175\_D\_vs\_C\_geneontology\_Molecular\_Function.txt.html

### Supplemental weblink-4 Gene Enrichment Report

file:///C:/Users/listerrl/AppData/Local/Temp/Rar\$EXa0.476/20190403\_rnaseq\_2499\_lister\_mouse\_placenta\_cutadapt/report/result/rnaseq\_Diabetic\_E175/enrichment\_results\_E175\_D\_vs\_C\_pathway\_KEGG.txt.html

### Supplemental weblink-5 Leica Imaging Hub- Digital files to all images

<http://ebcdih.mc.vanderbilt.edu/dih/browse.php?token=bkoxdU0ySUdNS1cyTUtXV01RMDBXejFpcUo1MEZKRDlad0x6TXo5Z-k1USWxGskQ5WkdWbVpHVm0tPS1aVEl6WWpZd1pEUmtOakZtTmpKbE1EaGpNREJpTWpkbU9UazFNRFZqTkRRd1IUVT-BPREE0Wmc9PQ==>